Article

Observational Constraints on $\mathcal{F}(\mathcal{T}, \mathcal{T}_{\mathcal{G}})$ Gravity with Hubble's Parametrization

Salim Harun Shekh [1,*] **, Nurgissa Myrzakulov** [2,3,†] **, Anirudh Pradhan** [4] **and Assem Mussatayeva** [2,5,†]

1   Department of Mathematics, S. P. M. Science and Gilani Arts, Commerce College, Ghatanji, Dist. Yavatmal, Maharashtra 445301, India
2   Department of General and Theoretical Physics, L N Gumilyov Eurasian National University, Astana 010008, Kazakhstan
3   Ratbay Myrzakulov Eurasian International Centre for Theoretical Physics, Astana 010009, Kazakhstan
4   Centre for Cosmology, Astrophysics and Space Science (CCASS), GLA University, Mathura 281406, India
5   Department of Physics and Chemistry, S. Seifullin Kazakh Agrotechnical University, Astana 010011, Kazakhstan
*   Correspondence: da_salim@rediff.com
†   These authors contributed equally to this work.

Abstract: Any new gravitational theories can be built with the help of a gauge theory with local Poincare symmetry. This local Poincare symmetry can set up a space-time with torsion. In the present study, the authors working on the parametrization approach towards Hubble's parameter in the frame of modified teleparallel Gauss-Bonnet gravity which is established on the torsion invariant $\mathcal{T}$ and the teleparallel equivalent of the Gauss-Bonnet term $\mathcal{T}_{\mathcal{G}}$, say $\mathcal{F}(\mathcal{T}, \mathcal{T}_{\mathcal{G}})$ gravity. In particular, gravity is responsible for an integrated explanation of the cosmological history from early-time inflation to late-time acceleration expansion, by lacking the addition of a cosmological constant. The domino effect acquired is reliable with recent cosmological outcomes. A transition scenario from a decelerating phase to an accelerating phase of cosmic evolution has been detected. Using the combined datasets (SNe-Ia+BAO+CMB+$H(z)$), we have constrained the transition redshift z_t (at which the universe transit from a decelerating phase to an accelerating) and established the best fit value of z_t. Next, we paralleled the renovated results of $q(z)$ and $\omega(z)$ and found that the outcomes are well-suited with a ΛCDM universe.

Keywords: FRW space-time; dark energy; $\mathcal{F}(\mathcal{T}, \mathcal{T}_{\mathcal{G}})$ gravity; cosmology

1. Introduction

Astronomical data and theoretical influences put forward that the cosmos passed through an early inflationary era and brought about an accelerated era at a late time [1–7]. The confirmations that have been specified to explain this stage can commonly be put into two categories. One way is to revise the universe content by bringing together additional fields such as canonical and non-canonical scalars, fermionic, etc., that make known the conceptions of the inflation and/or the dark energy (DE), which can be protracted in an enormous class of models see [8–10]. Moreover, DE is classified by the equation of state parameter (ω) which is defined as $\omega = \frac{p}{\rho}$. The equation of state parameter is not certainly constant but the inconstant time dependant equation of state parameter is responsible for more physically feasible and realistic DE models explored by the Chevallier-Polarski-Linder (CPL) parametrization [11,12]. If ω is slightly upper and lower than -1 then it would be respectively equal to the quintessence and phantom DE cosmology whereas the possibility $\omega << -1$ is ruled out by current cosmological data. Together with several additional restrictions of the equation of state parameter are obtained from SNe-Ia data and a combination of SNe-Ia data with CMB anisotropy and Galaxy clustering statistics are $-1.66 < \omega < -0.62$ and $-1.33 < \omega < -0.79$ correspondingly. The modern outcome

obtained from cosmological data sets coming from CMB anisotropy, luminosity distances of high red-shift SNe-Ia, and galaxy clustering constrain the range of ω lies in $-1.44 < \omega < -0.92$. Further, the CMB revealed that DE subsidizes 68% to the entire energy at the ease of the Universe. The cosmological constant Λ is the supreme up-front DE candidate with the equation of state $\omega = -1$. The ΛCDM model, containing the both cosmological constant (Λ) and cold dark matter (CDM), is the regular model that constantly fits with the current observational data sets. On the other hand, the Λ suffers from fine-tuning and coincidence matters. The other one is to transform the gravitational sector (Hilbert-Einstein action) instead which resulted in modified gravity theories. An extension of Hilbert-Einstein action leads to the $f(R)$ gravity [13–22] which represents a class of theories defined as arbitrary functions of R. An approach to transforming the gravitational Hilbert- Einstein action is to spread out the work of the corresponding torsion formulation, called *Teleparallel Equivalence of General Relativity* (TEGR) [23–26]. In this class of gravity, the Weitzenbock connection is used instead of the torsion-less Levi-Civita connection and the torsion scalar T can be achieved after the contraction of the torsion tensor. Torsional formulation of gravity plays an essential role in the so-called Poincare gauge gravity, where the Poincare invariance plays a fundamental role. Moreover, torsional gravities can be obtained starting from the local Poincare symmetry. In the Poincare approach, torsion contributes to the overall dynamics where internal degrees of freedom (spins) and external degrees of freedom (space-time). Furthermore, based on a nonlinear realization of the local conformal-affine group of symmetry transformations was formulated. A number of significant studies on the astrophysical as well as cosmological aspects of $f(\mathcal{T})$ gravity are ended in the references [27–37]. Other alternatives are $f(R, T)$ gravity [38–43], $f(R, L_m)$ gravity [44–49]. Another, in the teleparallel formulation of gravity, the complex curvature rectifications can be acquainted with the Gauss-Bonnet combination $\mathcal{G}$ in which the torsion invariant term $\mathcal{T}_{\mathcal{G}}$ has been pulling out without commanding the Weitzenbock connection [50–59], this lead to an alternative remarkable class of modified gravity, known as $\mathcal{F}(\mathcal{T}, \mathcal{T}_{\mathcal{G}})$ gravity [60,61]. These $\mathcal{F}(\mathcal{T}, \mathcal{T}_{\mathcal{G}})$ gravity have been broadly considered in several contexts and acquired an exciting domino effect on multiple scales [62–64]. By adding the matter sector along with the gravitational one, the total action for $\mathcal{F}(\mathcal{T}, \mathcal{T}_{\mathcal{G}})$ gravity is defined as [62],

$$S_{tot} = \frac{1}{2\kappa^2} \int \left(d^4 x e \mathcal{F}(\mathcal{T}, \mathcal{T}_{\mathcal{G}}) + S_m \right), \tag{1}$$

where S_m relates to a matter energy-momentum tensor and $\kappa^2 = 8\pi G$ be the four-dimensional Newton's constant.

Any model that just reduces the sound horizon recombination can never fully resolve the Hubble tension while still being consistent with other cosmological datasets, as shown by Jedamzik et al. [65] in their study. They have explicitly demonstrated that models with larger $\Omega_m h^2$ develop tension with galaxy-weak lensing data, whereas models with smaller $\Omega_m h^2$ develop tension with observations of baryon acoustic oscillations. This is because models with lower matter density $\Omega_m h^2$ achieve a higher Hubble constant.

Inspiring by the effective cosmological domino effect of $f(\mathcal{T})$ and the extension of $f(\mathcal{T})$ gravity, in this study, the author study a gravitational action of the torsion scalar and the Gauss-Bonnet component which omits the $\mathcal{F}(\mathcal{T}, \mathcal{T}_{\mathcal{G}})$ theory is considered. In particular, the author shall make an effort to the behavior of the Universe at the late time of its evolution.

The article is organized as follows: In Section 2. given basic formalism of $\mathcal{F}(\mathcal{T}, \mathcal{T}_{\mathcal{G}})$ theory. In Section 3. presented parametrization of the Hubble parameter. Basic observational constraints are shown in Section 4. and results of tests summarised Section 5. Interesting behavior of physical parameters graphically presented in Section 6. Conclusions in detail given in Section 7.

2. Cosmology with $\mathcal{F}(\mathcal{T}, \mathcal{T_G})$ Gravity

In order to inspect the astrophysical and cosmological implications of the action (1), here the author thinks through a spatially flat cosmological *ansatz* of the form

$$ds^2 = -N^2(t)dt^2 + a^2(t)\left(dx^2 + dy^2 + dz^2\right), \tag{2}$$

where $a(t)$ indicates the scale factor and $N(t)$ be the lapse function. This metric omits the diagonal vierbein and its determinant as

$$e^{\alpha}_{\mu} = diag(N, a, a, a), \quad \text{and} \quad e = Na^3 \tag{3}$$

As usual, consider $N(t) = 1$. Using the vierbein (3) of the considered cosmological *ansatz* (2), we found

$$\mathcal{T} = 6H^2 \quad \text{and} \quad \mathcal{T_G} = 24H^2(\dot{H} + H^2), \tag{4}$$

where $H = \dot{a}/a$ represents the Hubble's parameter and the overhead dot denotes the differentiation with respect to cosmic time t.

Furthermore, varying the action (1), the equations of motion using diagonal vierbein (3) are formed as [60,61],

$$2\kappa^2\rho = \mathcal{F} - 12H^2\mathcal{F_T} - \mathcal{T_G}\mathcal{F_{T_G}} + 24H^3\dot{\mathcal{F}}_{\mathcal{T_G}} \tag{5}$$

$$-2\kappa^2 p = \mathcal{F} - 4(\dot{H} + 3H^2)\mathcal{F_T} - 4H\dot{\mathcal{F}}_{\mathcal{T}} - \mathcal{T_G}F_{\mathcal{T_G}} + \frac{2\mathcal{T_G}\dot{\mathcal{F}}_{\mathcal{T_G}}}{3H} + 8H^2\ddot{\mathcal{F}}_{\mathcal{T_G}} \tag{6}$$

here $\mathcal{F} = \mathcal{F}(\mathcal{T}, \mathcal{T_G}), \mathcal{F_T} = \frac{\partial \mathcal{F}(\mathcal{T}, \mathcal{T_G})}{\partial \mathcal{T}}$ and $\mathcal{F_{T_G}} = \frac{\partial \mathcal{F}(\mathcal{T}, \mathcal{T_G})}{\partial \mathcal{T_G}}$.

To analyze the above components of the equation of motion, it is necessarily required to consider the form of $\mathcal{F} = \mathcal{F}(\mathcal{T}, \mathcal{T_G})$. Hence go through the utmost essential and non-trivial model of the form (which does not introduce a new mass scale into the problem),

$$\mathcal{F}(\mathcal{T}, \mathcal{T_G}) = -\mathcal{T} + \epsilon_1 f(\mathcal{T}, \mathcal{T_G}), \tag{7}$$

where $f(\mathcal{T}, \mathcal{T_G}) = \sqrt{(\mathcal{T}^2 + \epsilon_2 \mathcal{T_G})}$, ϵ_1 and ϵ_2 are dimensionless coupling model parameters. Also, the model is forecast to be necessary in late times. As, this model can yield significant cosmic behavior validating the advantages, opportunities, and original features of $\mathcal{F}(\mathcal{T}, \mathcal{T_G})$ cosmology [66].

In view of the $\mathcal{F}(\mathcal{T}, \mathcal{T_G})$ the model given in (7), and the components of equation of motion provided in Equations (5) and (6) become,

$$\kappa^2\rho = 6H^2\left(2 - \frac{\epsilon_1\left(2\mathcal{T_G}\epsilon_2\mathcal{T} + \dot{\mathcal{T}}_{\mathcal{G}}\epsilon_2^2 + 2\mathcal{T}^3\right)}{\left(\mathcal{T_G}\epsilon_2 + \mathcal{T}^2\right)^{3/2}}\right) + \frac{\epsilon_1\left(\mathcal{T_G}\epsilon_2 + 2\mathcal{T}^2\right)}{2\sqrt{\mathcal{T_G}\epsilon_2 + \mathcal{T}^2}} - \mathcal{T} \tag{8}$$

$$\kappa^2 p = 3H^2\left(\frac{\epsilon_1\left(4\mathcal{T}\left(\mathcal{T_G}\epsilon_2 + \mathcal{T}^2\right)^2 - \dot{\mathcal{T}}_{\mathcal{G}}^2\epsilon_2^3\right)}{\left(\mathcal{T_G}\epsilon_2 + \mathcal{T}^2\right)^{5/2}} - 4\right) + \frac{\mathcal{T_G}\dot{\mathcal{T}}_{\mathcal{G}}\epsilon_1\epsilon_2^2}{6H(\mathcal{T_G}\epsilon_2 + \mathcal{T}^2)^{3/2}} + \frac{4\mathcal{T_G}H\epsilon_1\epsilon_2\dot{\mathcal{T}}}{\left(\mathcal{T_G}\epsilon_2 + \mathcal{T}^2\right)^{3/2}}$$
$$+\dot{H}\left(\frac{4\epsilon_1\mathcal{T}}{\sqrt{\mathcal{T_G}\epsilon_2 + \mathcal{T}^2}} - 4\right) - \frac{\epsilon_1\left(\mathcal{T_G}\epsilon_2 + 2\mathcal{T}^2\right)}{2\sqrt{\mathcal{T_G}\lambda2 + \mathcal{T}^2}} + \mathcal{T} \tag{9}$$

3. Isotropization

To examine the changing aspects of models/dark energy models, there are several somatic arguments and inspirations for the model are present in the literature. In this section, the authors keep an eye on the similar idea of parametrization of cosmological models and explain the gravitational equations openly and study the dynamics in an altered phase of the universe's evolution. To define the phase transition of cosmological models

from early-time inflation and deceleration to acceleration in late time, various cosmologists have well-thought-out parametrization of cosmological parameters and constrained them through observational data. Most of them are equations of state, deceleration, Hubble's, and some well-known CPL parametrizations [67,68]. Hence, examine the parametrization of the Hubble parameter as

$$H(z) = \frac{H_0}{1 + \gamma}\left[1 + \frac{\gamma}{a^{1/\beta}}\right],$$ (10)

where a is the average scale factor, H_0 be the present value of $H(z)$, γ and β both are non-negative free model parameters. Using $(1 + z) = \frac{1}{a}$, one can represent the above Equation (10) in z as

$$H(z) = \frac{H_0}{1 + \gamma}\left[1 + \gamma(1 + z)^{1/\beta}\right].$$ (11)

4. Observational Constraints

In the previous sections, we have briefly described the $\mathcal{F}(\mathcal{T}, \mathcal{T}_\mathcal{G})$ gravity and solved the field equation with a new parametrization of the Hubble parameter. In order to extract the best fit values, the considered form of $H(z)$ was constrained by SNIa from Pantheon, CMB from Planck 2018, BAO, and 36 data points from Hubble. In what follows, we describe in detail the methodology adopted and data used in our analysis in the following subsections. The results of our study are shown in Tables 1 and 2 along with the contour plots (two-dimensional) with 1σ and 2σ errors.

Table 1. The table displays the mean values of the free cosmological parameters as well as their summary and best fit.

Model	Par	Prior	Best Fit	Mean
ΛCDM	Ω_{m}	[0.001, 1]	$0.311408^{+0.00589651}_{-0.00589651}$	$0.311568^{+0.0058866}_{-0.0058866}$
	$\Omega_{\mathrm{b}}h^2$	[0.001, 1]	$0.0223949^{+0.000131606}_{-0.000131606}$	$0.0224038^{+0.000131345}_{-0.000131345}$
	h	[0.4, 1]	$0.679136^{+0.00435014}_{-0.00435014}$	$0.679113^{+0.0043422}_{-0.0043422}$
Model	β	[0, 1]	$0.673644^{+0.00366388}_{-0.00366388}$	$0.673728^{+0.00366858}_{-0.00366858}$
	γ	[0, 1]	$0.62501^{+0.0000621386}_{-0.0000621386}$	$0.625011^{+0.00006221}_{-0.00006221}$
	h	[0.4, 1]	$0.657403^{+0.00408987}_{-0.00408987}$	$0.657422^{+0.00409376}_{-0.00409376}$

Table 2. The table shows the summary of $\chi^2_{tot}{}^{min}$, AIC_c and ΔAIC_c.

Model	$\chi^2_{tot}{}^{min}$	AIC_c	ΔAIC_c
ΛCDM	1102.2611	1108.28	0
Model	1108.2811	1109.4586	1.1771

4.1. Supernovae Type Ia (SNe-Ia)

Here, we use supernovae from Pantheon compilation made of 1048 spectroscopically confirmed Type Ia Supernovae distributed in the Redshift range $0.01 < z < 2.26$ [69]. So for the Pantheon compilation, the *chi-square* equation is expressed as

$$\chi^2_{SN} = (\mu_{obs} - \mu_{th})^T.C^{-1}_{Pan}.(\mu_{obs} - \mu_{th}),$$ (12)

where $\mu_{th} = 5\log_{10}\frac{cD_L}{H_0 Mpc} + 25$, μ_{obs} be the observed distance modulus and C_{Pan} is the covariance matrix of Pantheon data.

4.2. Cosmic Microwave Background

The χ^2 for cosmic microwave background is expressed as follows [70]

$$\chi^2_{\text{CMB}}(\beta, \gamma, h) = \mathbf{X}^{\mathbf{T}}_{\text{CMB}}(\beta, \gamma, h) . \mathbf{C}^{-1}_{\text{CMB}} . \mathbf{X}_{\text{CMB}}(\beta, \gamma, h), \tag{13}$$

where $\mathbf{X}^{\mathbf{T}}_{\text{CMB}}(\beta, \gamma, h) = (R(\beta, \gamma, h) - 1.74963, l_a(\beta, \gamma, h) - 301.80845, \Omega_{\text{b}} h^2(\beta, \gamma, h) - 0.02237)$ and $\mathbf{C}_{\text{CMB}}$ be the cosmic microwave background covariance matrix.

4.3. Baryon Acoustic Oscillation

In this paper, we use correlated BAO data (6dFGS, WiggleZ and Lya) and uncorrelated ones (SDSS DR7 MGS, BOSS-LOWZ, BOSS-DR12, BOSS-CMASS and DES) [71,72]. Hence, the total *chi-square* for BAO, χ^2_{BAO}, is expressed as

$$\chi^2_{BAO}(\beta, \gamma, h) = \chi^2_{6dFGS} + \chi^2_{SDSS} + \chi^2_{BOSS-LOWZ} + \chi^2_{BOSS-CMASS} + \chi^2_{WiggleZ} + \chi^2_{BOSS-DR12}. \tag{14}$$

The peak positions of Baryon Acoustic Oscillation are in general given in terms of $DV(z)/r_s(z)$, $DA(z)/r_s(z)$ and $H(z)/r_s(z)$ measured at the drag epoch z_{drag} i.e., where baryons were released from photons.

4.4. Hubble's Data

For the constraints, we also make use of the Hubble measurements $H(z)$. This observation can be regarded as cosmic chronometers, and we use a sample covering the redshift range $0 < z < 2.34$. For, these measurement the estimator χ^2 equation is expressed as:

$$\chi^2_{H(z)}(\beta, \gamma, h) = \sum_{i=1}^{36} \left[\frac{H_{obs,i} - H(z_i, \beta, \gamma, h)}{\sigma_{H,i}} \right]^2. \tag{15}$$

where H_{obs} be the observed value of $H(z)$ and $\sigma_H(z_i)$ represents the observational errors on the measured values $H_{obs}(z_i)$.

4.5. Monte Carlo Markov Chain (MCMC)

We can test the predictions of our theory with the available data by implementing the MCMC process. Hence, the total χ^2 defined as

$$\chi^2 = \chi^2_{SN} + \chi^2_{\text{CMB}} + \chi^2_{BAO} + \chi^2_{H(z)} \tag{16}$$

5. Results on Observational Tests

After successfully implementing the MCMC process, we got the best fit and mean values of the cosmological free parameters β, γ that appear in Table 1. Further, an exciting feature is perceived in the significance of the Hubble constant, well-defined as $H_0 = 100$ h. With respect to the values acquired by [73] and the one forecast by Planck, our end result for H_0 perfectly resembles the value of Planck. The constrained values of the free cosmological parameters γ and β are found to be as $\gamma = 0.62501^{+0.000062138}_{-000062138}$, $\beta = 0.67364^{+0.0036638}_{-0.0036638}$ (See Figure 1. Also compare the resultant values of χ^2_{tot}, AIC_c and ΔAIC_c with the standard ΛCDM model, and observed that our model is supported and perfectly consistent with the observations as $\Delta AIC_c < 2$ (See Table 2).
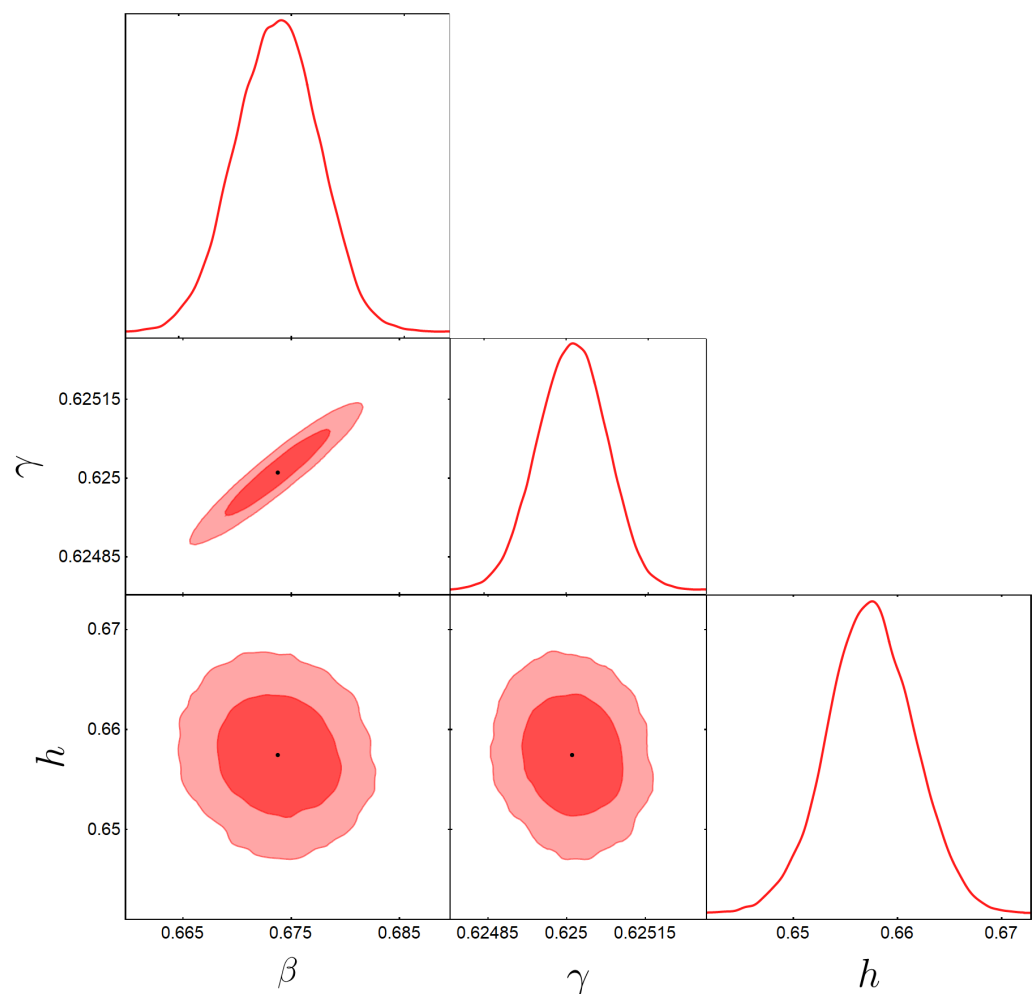
Figure 1. The figure shows the MCMC 1σ and 2σ confidence contours plot obtained from the combine SCBH dataset.

6. Physical Parameters

6.1. Deceleration Parameter

The deceleration parameter (DP) describes the rate of acceleration of the Universe and is defined as

$$q(z) = -1 - \frac{\dot{H}}{H^2} \tag{17}$$

The Universe is in a decelerating phase for optimistic $q > 0$, whereas an accelerating phase can be seen for unfavorable $q < 0$. Here, the model parameters γ and β both are cast-off to analyze the DP q. Figure 2, gives details of the expansion of transition from the past (positive) deceleration to the present (negative) acceleration for redshift z. At present, the DP is observed as $q_0 = -0.45015$ for the SNe-Ia+CMB+BAO+$H(z)$ (SCBH) dataset. Because of this, $q(z)$ at the current cosmic epoch is fairly compatible with the range $q_0 = -0.528^{+0.092}_{-0.088}$ as found by a recent observation [66,74].
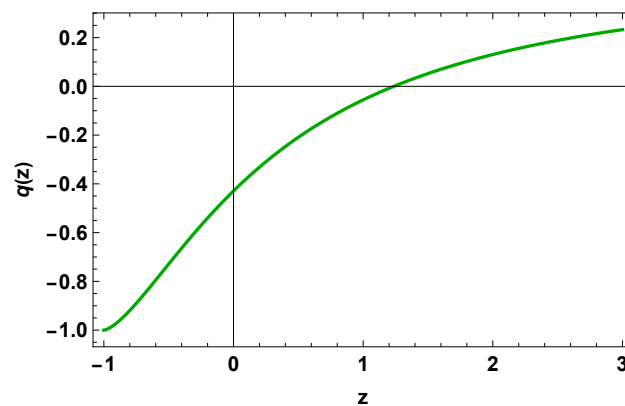
Figure 2. The DP with the best fit constraints value obtained from combined SCBH data versus redshift z.

6.2. Equation of State Parameter

When used to define the physical relevance of energy sources in the evolution of the universe, the equation of state (EoS) parameter is produced as

$$\omega = \frac{p}{\rho} = \frac{\left(\begin{array}{c} \mathcal{T} - \dfrac{3\dot{\mathcal{T}}_{\mathcal{G}}^2 H^2 \epsilon_1 \epsilon_2^3}{(\mathcal{G}\epsilon_2 + \mathcal{T}^2)^{5/2}} + \dfrac{\mathcal{T}_{\mathcal{G}} \dot{\mathcal{T}}_{\mathcal{G}} \epsilon_1 \epsilon_2^2}{6H(\mathcal{T}_{\mathcal{G}}\epsilon_2 + \mathcal{T}^2)^{3/2}} + 4\left(3H^2 + \dot{H}\right)\left(\dfrac{\epsilon_1 \mathcal{T}}{\sqrt{\mathcal{T}_{\mathcal{G}}\epsilon_2 + \mathcal{T}^2}} - 1\right) \\ + 4H\dot{\mathcal{T}}\left(\dfrac{\epsilon_1}{\sqrt{\mathcal{T}_{\mathcal{G}}\epsilon_2 + \mathcal{T}^2}} - \dfrac{\epsilon_1 \mathcal{T}^2}{(\mathcal{G}\epsilon_2 + \mathcal{T}^2)^{3/2}}\right) + \dfrac{\mathcal{T}_{\mathcal{G}}\epsilon_1\epsilon_2}{2\sqrt{\mathcal{T}_{\mathcal{G}}\epsilon_2 + \mathcal{T}^2}} - \epsilon_1\sqrt{\mathcal{T}_{\mathcal{G}}\epsilon_2 + \mathcal{T}^2} \end{array} \right)}{-\dfrac{6\dot{\mathcal{T}}_{\mathcal{G}}H^2\epsilon_1\epsilon_2^2}{(\mathcal{T}_{\mathcal{G}}\epsilon_2+\mathcal{T}^2)^{3/2}} - 12H^2\left(\dfrac{\epsilon_1\mathcal{T}}{\sqrt{\mathcal{T}_{\mathcal{G}}\epsilon_2+\mathcal{T}^2}} - 1\right) + \epsilon_1\sqrt{\mathcal{T}_{\mathcal{G}}\epsilon_2+\mathcal{T}^2} - \dfrac{\mathcal{T}_{\mathcal{G}}\epsilon_1\epsilon_2}{2\sqrt{\mathcal{T}_{\mathcal{G}}\epsilon_2+\mathcal{T}^2}} - \mathcal{T}} \tag{18}$$

The EoS parameter is characterized as follows:

- "For the dust phase the EoS parameter, $\omega = 0$,
- in the radiation-dominated phase, $\omega = \frac{1}{3}$,
- in the vacuum energy or ΛCDM model, the EoS parameter is recovered by $\omega = -1$.
- in the quintessence phase, EoS parameter lies in range $(-1 < \omega < 0)$,
- in the phantom regime $(\omega < -1)$".

In our investigation, the redshift-dependent behavior of the EoS parameter from Equation (13) is depicted in Figures 3 and 4 by taking into account the change in the values of ϵ_1 ($0.6681 \le \epsilon_1 \le 0.6881$) and ϵ_2 ($0.9851 \le \epsilon_2 \le 0.9951$). This picture indicates that the model approaches the ΛCDM limit at $z \to 0$ for all ϵ_2 and $\epsilon_1 = 0.6781$; this ΛCDM deviation also requires attention. It is usually convenient to have a ΛCDM limit to ensure that a model fits the data. The EoS parameter is constrained to have a range of $-1.02 \le \omega \le -0.986$ at the 1σ and 2σ confidence level for the collective dataset of the observations, whereas the best fit value is close to $\omega = -1.0024$ at the present epoch (see red color line in Figure 3) and it approaches -1 at late times (see Figures 3 and 4). As a result, we determine that the end result is almost reliable with the recent observational constraints on ω obtained by Wood-Vasey et al. [75] and Davis et al. [76] at $z \to 0$ and also in good agreement with the cosmological data Amanullah et al. [77] at $z \to -1$. Hence, we fix $\epsilon_1 = 0.6781$ and $\epsilon_2 = 0.9901$ throughout the analysis.
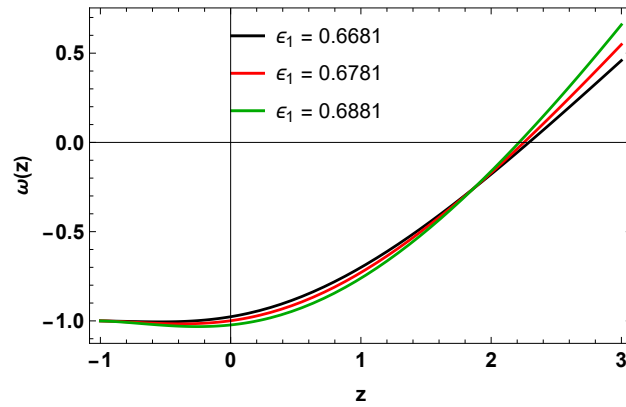
Figure 3. EoS parameter with the best fit constraints value obtained from SCBH data $\epsilon_1 = 0.6681$, $\epsilon_1 = 0.6781$ and $\epsilon_1 = 0.6881$ versus redshift z.
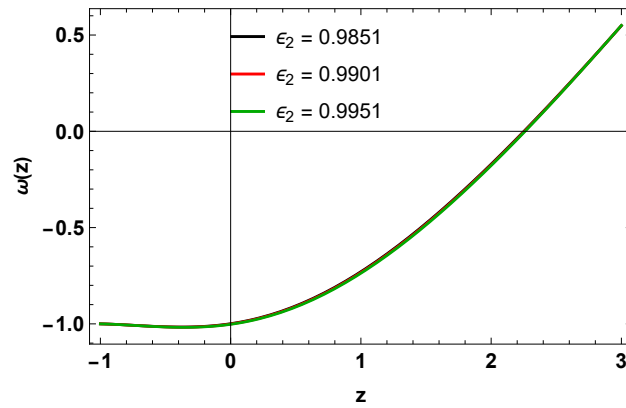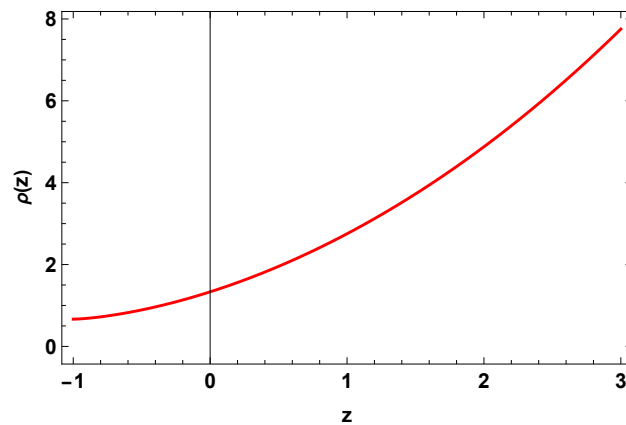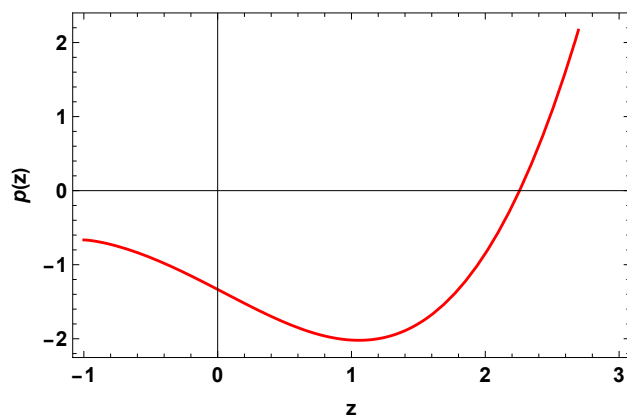

Figure 4. EoS parameter with the best fit constraints value obtained from SCBH data $\epsilon_2 = 0.9851$, $\epsilon_2 = 0.9901$ and $\epsilon_2 = 0.9951$ versus redshift z.

6.3. Energy Density and Pressure

With the best fit constraints value of β and γ which obtained from SCBH data and considered fix values of ϵ_1 and ϵ_2 the behavior of energy density and pressure is given in Figures 5 and 6.

Figure 5. Energy density of the Universe with the best fit constraints value obtained from SCBH data $\epsilon_1 = 0.6681$, $\epsilon_1 = 0.6781$ and $\epsilon_1 = 0.6881$ versus redshift z.

Figure 6. Isotropic pressure of the Universe with the best fit constraints value obtained from SCBH data $\epsilon_2 = 0.9851$, $\epsilon_2 = 0.9901$ and $\epsilon_2 = 0.9951$ versus redshift z.

The Figures 5 and 6 reveal that the redshift progression of energy density and isotropic pressure derived here in the framework of $\mathcal{F}(\mathcal{T}, \mathcal{T}_\mathcal{G})$ gravity is completely reliable with the outcomes resulting in more than a few works mentioned in the collected analysis [78–80]. In detail, the cosmic energy density is non-negative and increases with the redshift, despite the fact an isotropic pressure is negative at present and in the future. As a result, negative pressure is liable for the accelerating expansion of the Universe at present and in the future.

6.4. Energy Conditions

The energy conditions (EC) consent us to consider the behavior of gravitating systems without stipulating the detailed behavior of the matter. The well-known Raychaudhuri equation, which deals with appealing gravity, has shown to be highly helpful in describing energy conditions. Strong energy condition (SEC), weak energy condition (WEC), null energy condition (NEC), and dominant energy condition (DEC) are the four point-wise energy conditions that are limits on the stress-energy-momentum tensor of the matter that are most frequently utilized. In generally known that WEC is the most spontaneous of the energy conditions. The WEC implies $\rho \geq 0$ for a perfect fluid. Furthermore, the pressure of the universe can't be so negative it takes over the energy density, or $\rho + p \geq 0$. Next, the second law of black hole thermodynamics is determined by the null energy condition (NEC) [81–83]. Conferring to the meaning, we can also understand that if the NEC is violated, then the WEC and DEC on the other cannot be satisfied. In physical these energy conditions are defined as [84],

- "Null energy condition (NEC) $\iff \rho + p \geq 0$,
- Weak energy condition (WEC) $\iff \rho + p \geq 0$ and $\rho \geq 0$,
- Strong energy condition (SEC) $\iff \rho + p \geq 0$ and $\rho + 3p \geq 0$,
- Dominant energy condition (DEC) $\iff \rho - |p| \geq 0$ and $\rho \geq 0$".

The energy conditions in several modified theories of gravity are studied such as Capozziello [85] and Alvarenga [86] studied using the power law in $f(R)$ and $f(R, T)$ gravity, Liu [87] studied it with exponential as well as Born-Infeld $f(\mathcal{T})$ gravity, in $f(\mathcal{G})$ gravity by Garcia [88] and Bamba [89] also Atazadeh [90] investigated in $f(R, \mathcal{G})$ gravity. The energy conditions in cosmological models with variable anisotropic parameters in $f(R, T)$ gravity have been examined by Mishra et al. [91].

The plots of the energy conditions are presented in Figure 7. We can see from the figure that the model's NEC and DEC hold true, but the SEC is violated, which clearly indicates that the universe has accelerated expansion.
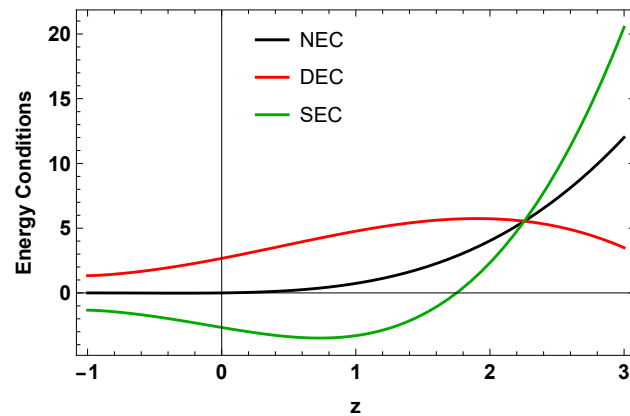
Figure 7. EC of the Universe with the best fit constraints value obtained from SCBH data $\epsilon_1 = 0.6681$, $\epsilon_1 = 0.6781$ and $\epsilon_1 = 0.6881$ versus redshift z.

7. Conclusions

In the present work the investigation of observational constraints towards a modified gravity based on the torsion scalar $(\mathcal{T})$ and the teleparallel equivalent of the Gauss-Bonnet combination $(\mathcal{T}_\mathcal{G})$ say $\mathcal{F}(\mathcal{T}, \mathcal{T}_\mathcal{G})$ gravity is presented. Firstly, the author takes out the general Friedmann equations and then, choosing specific $\mathcal{F}(\mathcal{T}, \mathcal{T}_\mathcal{G})$ *ansatzes* we executed a complete study of various observable, such as energy density, the equation of state parameters, etc. The consequential cosmology leads to motivating behaviors.

- A geometrical Hubble's parameter H parametrization has been deliberated using the best fit constraints values of free parameters β and γ obtained from SCBH data. This parametrization generates a time-dependent q and gives details the current accelerated expansion of the Universe, i.e., $q < 0$ with a prior deceleration, i.e., $q > 0$. Additionally, it is noted that the model deviates from the typical big bang scenario. The model with q as time-dependent has a signature flipping behavior with evolution. So, the feature of an early deceleration to the late acceleration of the model is appropriate for structure formation in the early stage of evolution and accelerated expansion in the later stage of the evolution.

- Also discovered that the free cosmological parameters that are included in $H(z)$ more specifically, could be associated in some way with the background parameters Ω_m and Ω_r. To end with, an exciting result here to comment on is that the value achieved for the Hubble parameter H_0, lies close to the Planck estimation.

- The behavior of energy density and pressure can be completely predicted using the best fit constraints values of β and γ, which were obtained from SCBH data and taken into consideration fix values of ϵ_1 and ϵ_2. The results have been reported in a number of works. In detail, the cosmic energy density is non-negative and increases with the redshift, despite the fact an isotropic pressure is negative at present and in the future. As a result, negative pressure is liable for the accelerating expansion of the Universe at present and in the future.

- In the analysis it is detected that the NEC and DEC both energy conditions are held, meanwhile, the SEC violates, the violation of SEC direct leads to the accelerating expansion of the Universe. Also, the WEC is non-negative from the early to late time phase of the Universe. Hence, the model reveals quintessential behavior. Simultaneously, the SEC was violated at a late time and satisfied at the early times (Figure 7).

Author Contributions: S.H.S.: Conceptualization, writing—review & editing, Programming, Investigation. N.M.: Writing—original draft, writing-review, editing. A.P.: Writing-original draft, Writing—review, editing, programming. A.M.: writing—review, editing. All authors have read and agreed to the published version of the manuscript.

Conflicts of Interest: The authors declare no conflict of interest.

References

1. Perlmutter, S.; Aldering, G.; Goldhaber, G.; Knop, R.A.; Nugent, P.; Castro, P.G.; Deustua, S.; Fabbro, S.; Goobar, A.; Groom, D.E.; et al. Measurements of Ω and Λ from 42 high-redshift supernovae. *Astrophys. J.* **1999**, *517*, 565–586.
2. Perlmutter, S.; Aldering, G.; Valle, M.D.; Deustua, S.; Ellis, R.S.; Fabbro, S.; Fruchter, A.; Goldhaber, G.; Groom, D.E.; Hook, I.M.; et al. Discovery of a supernova explosion at half the age of the Universe. *Nature* **1998**, *91*, 51.
3. Riess, A.G. The case for an accelerating universe from supernovae. *Astron. Soci. Pac.* **2000**, *112*, 1284.
4. Tonry, J.L.; Schmidt, B.P.; Barris, B.; Candia, P.; Challis, P.; Clocchiatti, A.; Coil, A.L.; Filippenko, A.V.; Garnavich, P.; Hogan, C.; et al. Cosmological results from high-z supernovae. *Astrophys. J.* **2003**, *94*, 1.
5. de Bernardis, P.; Ade, P.A.; Bock, J.J.; Bond, J.R.; Borrill, J.; Boscaleri, A.; Coble, K.; Crill, B.P.; De Gasperis, G.; Farese, P.C.; et al. A flat Universe from high-resolution maps of the cosmic microwave background radiation. *Nature* **2000**, *404*, 955–959. [CrossRef]
6. Spergel, D.N.; Verde, L.; Peiris, H.V.; Komatsu, E.; Nolta, M.R.; Bennett, C.L.; Halpern, M.; Hinshaw, G.; Jarosik, N.; Kogut, A.; et al. First-year Wilkinson Microwave Anisotropy Probe (WMAP)* observations: Determination of cosmological parameters. *Astrophys. J. Suppl. Ser.* **2003**, *148*, 175–194. [CrossRef]
7. Tegmark, M.; Strauss, M.A.; Blanton, M.R.; Abazajian, K.; Dodelson, S.; Sandvik, H.; Wang, X.; Weinberg, D.H.; Zehavi, I.; Bahcall, N.A.; et al. Cosmological parameters from SDSS and WMAP. *Phys. Rev. D* **2004**, *69*, 103501.
8. Bassett, B.A.; Tsujikawa, S.; Wands, D. Inflation dynamics and reheating. *Rev. Mod. Phys.* **2006**, *78*, 537. [CrossRef]
9. Copeland, E.J.; Sami, M.; Tsujikawa, S. Dynamics of dark energy. *Int. J. Phys. D* **2006**, *15*, 1753–1935.
10. Cai, Y.F.; Saridakis, E.N.; Setare, M.R.; Xia, J.Q. Quintom cosmology: Theoretical implications and observations. *Phys. Rep.* **2010**, *493*, 1–60. [CrossRef]
11. Chevallier, M.; Polarski, D. Accelerating universes with scaling dark matter. *Int. J. Mod. Phys. D* **2001**, *10*, 213–223. [CrossRef]
12. Linder, E.V. Exploring the expansion history of the universe. *Phys. Rev. Lett.* **2003**, *90*, 091301. [CrossRef]
13. Nojiri, S.I.; Odintsov, S.D. Modified f (R) gravity unifying R^m inflation with the ΛCDM epoch. *Phys. Rev. D* **2008**, *77*, 026007. [CrossRef]
14. Inagaki, T.; Taniguchi, M. Cartan $F(R)$ gravity and equivalent scalar-tensor theory. *Symmetry* **2022**, *14*, 1830. [CrossRef]
15. Ali, S.; Saif, M.; Khan, K.A.; Shah, N.A. A note on varying G and Λ in Chern-Simons modified gravity. *Symmetry* **2022**, *14*, 1430. [CrossRef]
16. Bekov, S.; Myrzakulov, K.; Myrzakulov, R.; Gomez, S.-C. General slow-roll inflation in $f(R)$ gravity under the Palatini approach. *Symmetry* **2020**, *12*, 1958. [CrossRef]
17. Granda, L. Unified inflation and late-time accelerated expansion with exponential and R^2 corrections in modified gravity. *Symmetry* **2020**, *12*, 749. [CrossRef]
18. Godani, N. Thin-shell wormhole solution in $f(R)$ gravity. *New Astron.* **2023**, *98*, 101941.
19. Nojiri, S.I.; Odintsov, S.D. Unified cosmic history in modified gravity: From F (R) theory to Lorentz non-invariant models. *Phys. Rept.* **2011**, *505*, 59–144.
20. Capozziello, S.; De Laurentis, M. Extended theories of gravity. *Phys. Rep.* **2011**, *509*, 167–332.
21. Odintsov, S.D.; Oikonomou, V.K. Early-time cosmology with stiff era from modified gravity. *Phys. Rev. D* **2017**, *6*, 104059.
22. Odintsov, S.D.; Oikonomou, V.K. Reconstruction of slow-roll F (R) gravity inflation from the observational indices. *Ann. Phys.* **2018**, *388*, 267–275. [CrossRef]
23. Einstein, A. Riemann-Geometrie mit Aufrechterhaltung des Begriffes des Fernparallelismus, Neue Möglichkeit für eine einheitliche Feldtheorie von Gravitation und Elektrizität. *Sitzungsber. Preuss. Akad. Wiss. Berl. Phys. Math.* **1928**, *Kl*, 224.
24. Arcos, H.I.; Pereira, J.G. Torsion gravity: A reappraisal. *Int. J. Mod. Phys. D* **2004**, *13*, 2193–2240. [CrossRef]
25. Maluf, J.W. The teleparallel equivalent of general relativity. *Ann. Phys.* **2013**, *525*, 339–357.
26. Aldrovandi, R.; Pereira, J.G. *Teleparallel Gravity: An Introduction*; Springer: Dordrecht, The Netherlands, 2013.
27. Capozziello, S.; Cardone, V.F.; Farajollahi, H.; Ravanpak, A. Cosmography in f (T) gravity. *Phys. Rev. D* **2011**, *84*, 043527.
28. Myrzakulov, R. Accelerating universe from F (T) gravity. *Eur. Phys. J. C* **2011**, *71*, 1752.

29. Jeon, I.; Lee, K.; Park, J.H. Differential geometry with a projection: Application to double field theory. *J. High Energy Phys.* **2011**, *2011*, 14. [CrossRef]

30. Tamanini, N.; Boehmer, C.G. Good and bad tetrads in f (T) gravity. *Phys. Rev. D* **2012**, *86*, 044009.

31. Cai, Y.F.; Capozziello, S.; De Laurentis, M.; Saridakis, E.N. f (T) teleparallel gravity and cosmology. *Rep. Prog. Phys.* **2016**, *9*, 106901.

32. Anagnostopoulos, F.K.; Basilakos, S.; Saridakis, E.N. Bayesian analysis of f (T) gravity using $f\sigma_8$ data. *Phys. Rev. D* **2019**, *100*, 083517.

33. Nair, K.K.; Arun, M.T. Kalb-Ramond field-induced cosmological bounce in generalized teleparallel gravity. *Phys. Rev. D* **2022**, *105*, 103505. [CrossRef]

34. Shekh, S.H.; Chirde, V.R. Accelerating Bianchi type dark energy cosmological model with cosmic string in f(T) gravity. *Astrophys. Space Sci.* **2020**, *365*, 1–10. [CrossRef]

35. Chirde, V.R.; Shekh, S.H. Analysis of general relativistic hydrodynamic cosmological models with stability factor in theories of gravitation. *Gen. Relativ. Gravit.* **2019**, *51*, 87.

36. Chirde, V.R.; Shekh, S.H. Dynamic minimally interacting holographic dark energy cosmological model in $f(T)$ gravity. *Indian J. Phys.* **2018**, *92*, 1485.

37. Bhoyar, S.R.; Chirde, V.R.; Shekh, S.H. Stability of accelerating universe with a linear equation of state in $f(T)$ gravity using hybrid expansion law. *Astrophysics* **2017**, *60*, 259–272. [CrossRef]

38. Zubair, M.; Zeeshan, M.; Hasan, S.S.; Oikonomou, V.K. Impact of Collisional Matter on the Late-time Dynamics of $f(R,T)$ gravity. *Symmetry* **2018**, *10*, 463. [CrossRef]

39. Hulke, N.; Singh, G.P.; Bishi, B.K.; Singh, A. Variable chaplygin gas cosmologies in $f(R,T)$ gravity with particle creation. *New Astron.* **2020**, *77*, 101357. [CrossRef]

40. Sharma, U.K.; Kumar, M.; Varshney, G. Scalar field for Barrow holographic dark energy in $f(R,T)$ gravity. *Universe* **2022**, *8*, 642.

41. Mishra, A.K.; Sharma, U.K. Wormhole models in R^2-fravity for $f(R,T)$ theory with a hybrid shape function. *Can. J. Phys.* **2021**, *99*, 481–489.

42. Pretel, J.M.Z.; Tangphati, T.; Banerjee, A.; Pradhan, A. Charged Quark Stars in $f(R,T)$ Gravity. *Chin. Phys. C* **2022**, *46*, 115103. [CrossRef]

43. Tangphati, T.; Hansraj, S.; Banerjee, A.; Pradhan, A. Quark stars in $f(R,T)$ gravity with an interacting quark equation of state. *Phys. Dark Univ.* **2022**, *35*, 100990. [CrossRef]

44. Harko, T.; Lobo, F.S.N. $f(R,L_m)$ gravity. *Eur. Phys. J. C* **2010**, *70*, 373–379. [CrossRef]

45. Faraoni, V. *Cosmology in Scalar-Tensor Gravity*; Kluwer Academic: Dordrecht, The Netherlands, 2004.

46. Bertolami, O.; Piramos, J.; Turyshev, S. *General Theory of Relativity: Will It Survive the Next Decade?* Springer: Berlin/Heidelberg, Germany, 2008; pp. 27–74.

47. Wang, J.; Liao, K. Energy conditions in $f(R,L_m)$ gravity. *Class. Quantum Gravity* **2012**, *29*, 215016.

48. Pradhan, A.; Maurya, D.C.; Goswami, G.K.; Beesham, A. Modeling transit dark energy in $f(R,L_m)$ gravity. *arXiv* **2022**, arXiv:2209.14269. [CrossRef]

49. Lakhan, V.J.; Solanki, R.; Mandal, S.; Sahoo, P.K. Cosmology in $f(R,L_m)$ gravity. *Phys. Lett. B* **2022**, *831*, 137148.

50. Boulware, D.G.; Deser, S. String-generated gravity models. *Phys. Rev. Lett.* **1985**, *55*, 2656. [CrossRef]

51. Nojiri, S.I.; Odintsov, S.D.; Sasaki, M. Gauss-Bonnet dark energy. *Phys. Rev. D* **2005**, *71*, 123509.

52. Rodrigues, M.E.; Houndjo, M.J.S.; Momeni, D.; Myrzakulov, R. A type of Levi–Civita solution in modified Gauss-Bonnet gravity. *Can. J. Phys.* **2014**, *92*, 173. [CrossRef]

53. Tangphati, T.; Pradhan, A.; Errehymy, A.; Banerjee, A. Quark Stars in the Einstein-Gauss-Bonnet theory: A New Branch of Stellar Configurations. *Ann. Phys.* **2021**, *430*, 168498.

54. Tangphati, T.; Pradhan, A.; Frrehymy, A.; Banerjee, A. Anisotropic quark stars in Einstein-Gauss-Bonnet theory. *Phys. Lett. B* **2021**, *819*, 136423. [CrossRef]

55. Tangphati, T.; Pradhan, A.; Banerjee, A.; Panotopoulos, G. Anisotropic Stars in 4D Einstein-Gauss-Bonnet Gravity. *Phys. Dark Univ.* **2021**, *33*, 100877.

56. Panotopoulos, G.; Pradhan, A.; Tangphati, T.; Banerjee, A. Charged Polytropic Compact Stars in 4D Einstein-Gauss-Bonnet Gravity. *Chin. J. Phys.* **2022**, *77*, 2106–2114.

57. Naicker, S.; Maharaj, S.D.; Brasel, B.P. Isotropic perfect fluids in modified gravity. *Universe* **2023**, *9*, 47. [CrossRef]

58. Shekh, S.H.; Katore, S.D.; Chirde, V.R.; Raut, S.V. Signature flipping of isotropic homogeneous space-time with holographic dark energy in $f(G)$ gravity. *New Astron.* **2020**, *84*, 101535.

59. Shekh, S.H. Dynamical analysis with thermodynamic aspects of anisotropic dark energy bounce cosmological model in $f(R,G)$ gravity. *New Astron.* **2021**, *83*, 101464.

60. Kofinas, G.; Saridakis, E.N. Teleparallel equivalent of Gauss-Bonnet gravity and its modifications. *Phys. Rev. D* **2014**, *90*, 084044. [CrossRef]

61. Kofinas, G.; Saridakis, E.N. Cosmological applications of $F(T,T_G)$ gravity. *Phys. Rev. D* **2014**, *90*, 084045. [CrossRef]

62. Kofinas, G.; Leon, G.; Saridakis, E.N. Dynamical behavior in $f(T,T_G)$ cosmology. *Class. Quantum Grav.* **2014**, *31*, 175011.

63. Chattopadhyay, S.; Jawad, A.; Momeni, D.; Myrzakulov, R. Pilgrim dark energy in $f(T,T_G)$ cosmology. *Astrophys. Space Sci.* **2014**, *53*, 279–292.

64. Capozziello, S.; De Laurentis, M.; Dialektopoulos, K.F. Noether symmetries in Gauss-Bonnet-teleparallel cosmology. *Eur. Phys. J. C* **2016**, *76*, 1–6. [CrossRef] [PubMed]

65. Jedamzik, K.; Pogosian, L.; Zhao, G.B. Why reducing the cosmic sound horizon alone can not fully resolve the Hubble tension. *Commun. Phys.* **2021**, *4*, 123.

66. Lohakare, S.V.; Mishra, B.; Maurya, S.K.; Singh, K. Constraining the cosmological parameters of modified Teleparallel-Gauss-Bonnet model. *arXiv* **2022**, arXiv:2209.13197.

67. Linder, E.V. Mapping the dark energy equation of state. In *Symposium-International Astronomical Union*; Cambridge University Press: Cambridge, UK, 2005; Volume 216, pp. 59–66.

68. Cunha, J.V.; Lima, J.A.S. Transition redshift: New kinematic constraints from supernovae. *Mon. Not. R. Astron. Soc.* **2008**, *390*, 210–217.

69. Scolnic, D.M.; Jones, D.O.; Rest, A.; Pan, Y.C.; Chornock, R.; Foley, R.J.; Huber, M.E.; Kessler, R.; Narayan, G.; Riess, A.G.; et al. The Complete Light-curve Sample of Spectroscopically Confirmed SNe Ia from Pan-STARRS1 and Cosmological Constraints from the Combined Pantheon Sample. *Astrophys. J.* **2018**, *859*, 101.

70. Zhai, Z.; Wang, Y. Robust and model-independent cosmological constraints from distance measurements. *J. Cosmol. Astropart. Phys.* **2019**, *1907*, 005. [CrossRef]

71. Anderson, L.; Aubourg, E.; Bailey, S.; Beutler, F.; Bhardwaj, V.; Blanton, M.; Bolton, A.S.; Brinkmann, J.; Brownstein, J.R.; Burden, A.; et al. [BOSS Collaboration], The clustering of galaxies in the SDSS-III Baryon Oscillation Spectroscopic Survey: Baryon acoustic oscillations in the Data Releases 10 and 11 Galaxy samples. *Mon. Not. R. Astron. Soc.* **2014**, *441* 24–62. [CrossRef]

72. Alam, U.; Bag, S.; Sahni, V. Constraining the Cosmology of the Phantom Brane using Distance Measures. *Phys. Rev. D* **2017**, *95*, 023524.

73. Riess, A.G.; Casertano, S.; Yuan, W.; Macri, L.M.; Scolnic, D. Large Magellanic Cloud Cepheid standards provide a 1% foundation for the determination of the Hubble constant and stronger evidence for physics beyond ΛCDM. *Astrophys. J.* **2019**, *876*, 85.

74. Gruber, C.; Luongo, O. Cosmographic analysis of the equation of state of the universe through Pade approximations. *Phys. Rev. D* **2014**, *89*, 103506.

75. Wood-Vasey, W.M.; Miknaitis, G.; Stubbs, C.W.; Jha, S.; Riess, A.G.; Garnavich, P.M.; Kirshner, R.P.; Aguilera, C.; Becker, A.C.; Blackman, J.W.; et al. Observational constraints on the nature of dark energy: First cosmological results from the essence supernova survey. *Astrophys. J.* **2007**, *666*, 694.

76. Davis, T.M.; Mortsell, E.; Sollerman, J.; Becker, A.C.; Blondin, S.; Challis, P.; Clocchiatti, A.; Filippenko, A.V.; Foley, R.J.; Garnavich, P.M.; et al. Scrutinizing exotic cosmological models using ESSENCE supernova data combined with other cosmological probes. *Astrophys. J.* **2007**, *66*, 716. [CrossRef]

77. Amanullah, R.; Lidman, C.; Rubin, D.; Aldering, G.; Astier, P.; Barbary, K.; Burns, M.S.; Conley, A.; Dawson, K.S.; Deustua, S.E.; et al. Spectra and Hubble Space Telescope light curves of six type Ia supernovae at $0.511 < z < 1.12$ and the Union2 compilation. *Astrophys. J. Lett.* **2010**, *716*, 712.

78. Shekh, S.H. Models of holographic dark energy in f (Q) gravity. *Phys. Dark Univ.* **2013**, *33*, 100850.

79. Koussour, M.; Filali, H.; Shekh, S.H.; Bennai, M. Holographic dark energy in Gauss-Bonnet gravity with Granda-Oliveros cut-off. *Nucl. Phys. B* **2022**, *978*, 115738. [CrossRef]

80. Shekh, S.H.; Moraes, P.H.; Sahoo, P.K. Physical acceptability of the renyi, tsallis and sharma-mittal holographic dark energy models in the f (t, b) gravity under hubble's cutoff. *Universe* **2021**, *7*, 67.

81. Wald, R.M. *General Relativity*; University of Chicago Press: Chicago, IL, USA, 1984.

82. Santos, J.; Alcaniz, J.S.; Reboucas, M.J.; Carvalho, F.C. Energy conditions in f (R) gravity. *Phys. Rev. D* **2007**, *76*, 083513.

83. Xu, Y.; Harko, T.; Shahidi, S.; Liang, S.D. Weyl type f (Q, T) gravity, and its cosmological implications. *Eur. Phys. J. C* **2020**, *80*, 1–22. [CrossRef]

84. Bouhmadi-Lopez, M.; Errahmani, A.; Martin-Moruno, P.; Ouali, T.; Tavakoli, Y. The little sibling of the big rip singularity. *Int. J. Mod. Phys. D* **2015**, *24*, 1550078. [CrossRef]

85. Capozziello, S.; Nojiri, S.I.; Odintsov, S.D. The role of energy conditions in f (R) cosmology. *Phys. Lett. B* **2018**, *781*, 99–106.

86. Alvarenga, F.G.; Houndjo, M.J.S.; Monwanou, A.V.; Orou, J.B.C. f (R, T) gravity from null energy condition. *Int. J. Mod. Phys.* **2013**, *4*, 130–139.

87. Liu, D.; Reboucas, M.J. Energy conditions bounds on f (T) gravity. *Phys. Rev. D* **2012**, *86*, 083515.

88. Garcia, N.M.; Harko, T.; Lobo, F.S.; Mimoso, J.P. Energy conditions in modified Gauss-Bonnet gravity. *Phys. Rev. D* **2011**, *83*, 104032. [CrossRef]

89. Bamba, K.; Ilyas, M.; Bhatti, M.Z.; Yousaf, Z. Energy conditions in modified f (G) gravity. *Gen. Relativ. Gravit.* **2017**, *49*, 1–17.

90. Atazadeh, K.; Darabi, F. Energy conditions in $f(R, G)$ gravity. *Gen. Relativ. Gravit.* **2014**, *46*, 1–14. [CrossRef]

91. Mishra, B.; Esmeili, F.M.; Ray, S. Cosmological Models with Variable Anisotropic Parameter in $f(R, T)$ Gravity. *Indian J. Phys.* **2021**, *95*, 2245–2254. [CrossRef]